Electronic Supplementary Material (ESI) for Journal of Materials Chemistry C.
This journal is © The Royal Society of Chemistry 2022

This updated document was made available online on 21st July 2022, it contains corrections to m* values in Fig. S14.

Supporting Information for

"Heavy-atom Effects" in the Parent [1]Benzochalcogenopheno[3,2-*b*][1] benzochalcogenophene System

Chengyuan Wang,[a] Mamatimin Abbas,[b] Guillaume Wantz,[b] Kohsuke Kawabata,[a,c] Kazuo Takimiya*,[a,c]

[a] Emergent Molecular Function Research Team, RIKEN Center for Emergent Matter Science (CEMS), 2-1 Hirosawa, Wako, Saitama 351-0198, Japan

[b] Univ. Bordeaux, IMS, CNRS, UMR-5218, Bordeaux INP, ENSCBP, 33405 Talence, France

[c] Department of Chemistry, Graduate School of Science, Tohoku University, 6-3 Aoba, Aramaki, Aoba-ku, Sendai, Miyagi 980-8578, Japan

Contents

1. Methods and Instruments

Single-crystal X-ray analysis of BTeBTe (CCDC: 1908813) was carried out on a Rigaku R-AXIS RAPID (Mo*K*α radiation, *λ* = 0.7108 Å, multilayer confocal optics). The structure was solved by direct methods. Non-hydrogen atoms were refined anisotropically, and hydrogen atoms were included in the calculations but not refined. All calculations were performed using the crystallographic software package CrystalStructures 4.2.[S1] UV-Vis spectra were recorded on a Shimadzu UV-3600 spectrometer. Cyclic voltammograms (CVs) were recorded on a ALS Electrochemical Analyzer Model 612D in benzonitrile solution containing tetrabutylammonium hexafluorophosphate (Bu_4NPF_6, 0.1 M) as the supporting electrolyte at a scanning rate of 100 mV/s. Pt was used as working and counter electrodes, and Ag/AgCl was used as the reference electrode. Ferrocene/ferrocenium redox couple (Fc/Fc^+) was used as external reference. Differential scanning calorimetry (DSC) were carried out on a Shimadzu DSC-60. Out-of-plane X-Ray Diffractions (XRD) patterns were obtained with a Rigaku Ultima IV diffractometer with a Cu*K*α source (λ = 1.541 Å) in air. Ionization potentials (IPs) of BTBT, BSBS, and BTeBTe in the solid state were evaluated by photoelectron spectroscopy in the air (PESA) on a RIKEN-Keiki AC-2 PESA instrument.

2. Device configurations

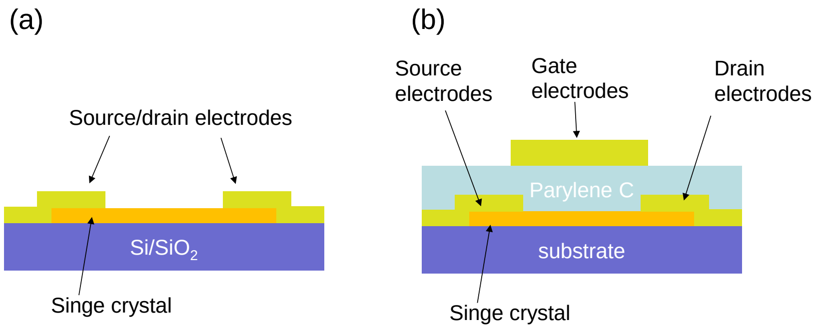

Fig. S1 Device configurations of single-crystal organic field-effect transistors (SC-OFETs) used in this study; (a) bottom-gate top-contact (BGTC) and (b) top-gate top-contact (TGTC).

3. Calculated HOMO and LUMO of BTBT, BSBS, and BTeBTe

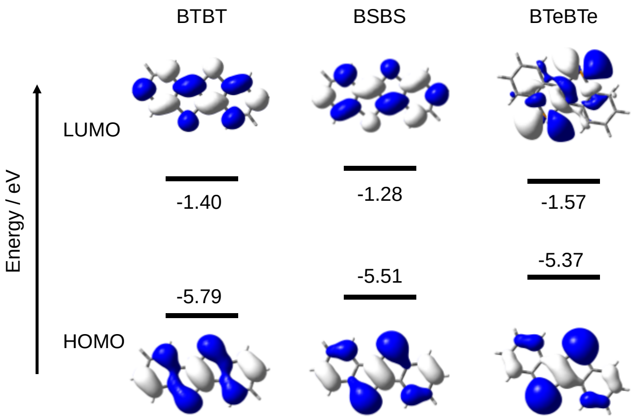

Fig. S2 HOMO and LUMO coefficients and energy levels of BTBT, BSBS, and BTeBTe calculated at B3LYP/3-21g level.

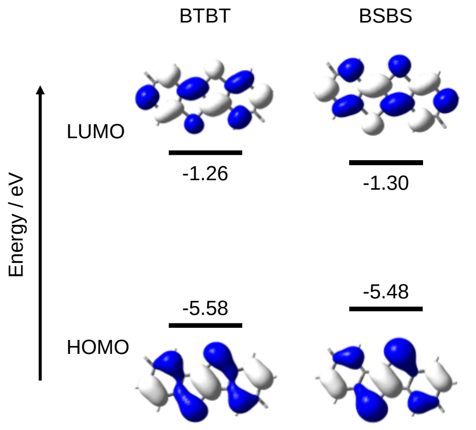

Fig. S3 HOMO and LUMO coefficients and energy levels of BTBT and BSBS calculated at B3LYP/6-31g(d) level.

4. DSC traces of BTBT, BSBS, and BTeBTe

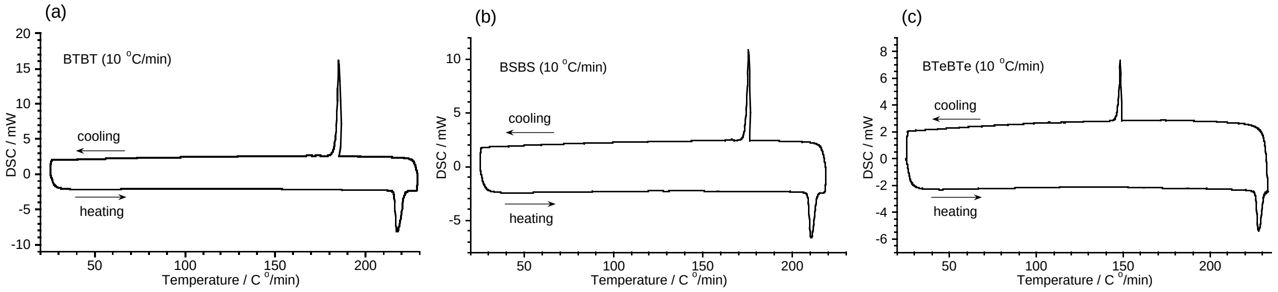

Fig. S4 Differential scanning calorimetry (DSC) curves of (a) BTBT, (b) BSBS, and (c) BTeBTe at the rate of 10 °C min^{-1}.

5. XRD of vapor-deposited thin film of BTeBTe on Si/SiO$_2$ substrate

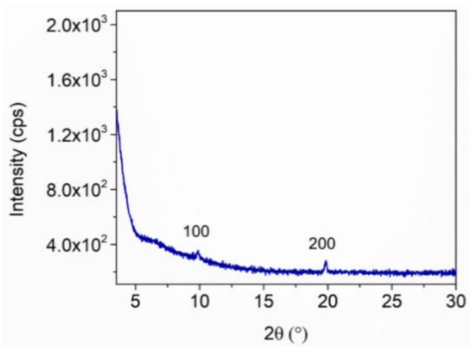

Fig. S5 Out-of-plane XRD patterns of the BTeBTe thin films deposited by vacuum deposition method.

6. XRD of BXBX singe crystals laminated on Si/SiO$_2$ substrate

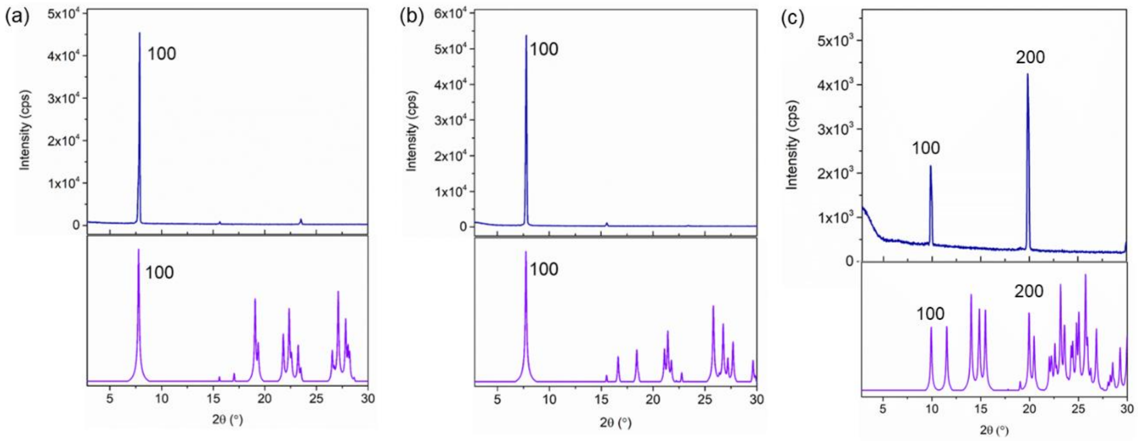

Fig. S6 Out-of-plane XRD patterns of the BXBX single crystals on the ODTS-modified Si/SiO$_2$ substrate (a) BTBT, (b) BSBS, (c) BTeBTe; top is the experimental data and bottom is the simulated patterns from single crystal data.

7. Determination of channel directions for single crystals of BXBXs

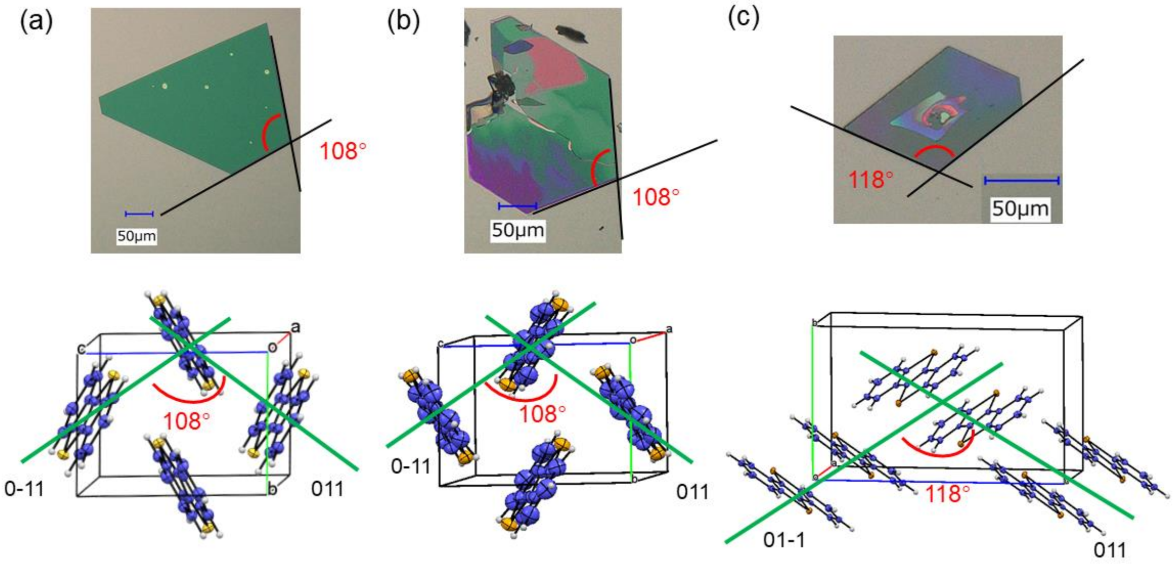

Fig. S7 Facets of the BXBX single crystals and the corresponding molecular organizations (a) BTBT, (b) BSBS, and (c) BTeBTe.

8. Device characteristics of Top-gate bottom-contact SC-OFETs of BTBT and BSBS.

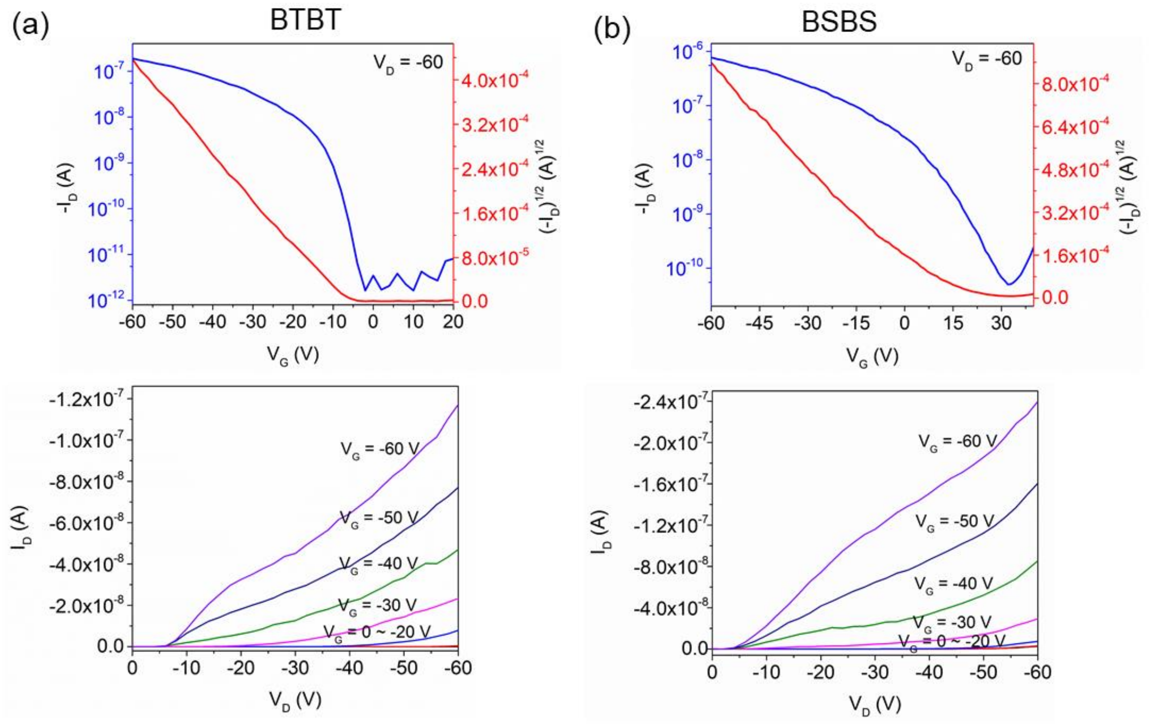

Fig. S8 Transfer (top) and output (bottom) curves of the BXBX-based TGBC SC-OFETs (a) BTBT, (b) BSBS.

9. NICS (Nucleus-Independent Chemical Shifts) calculations

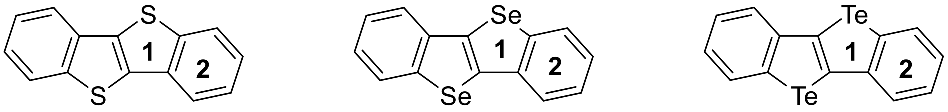

3-21g
NICS(0) **1**: -7.92, **2**: -9.07
NICS(1) **1**: -7.26, **2**: -10.89

6-31g(d)
NICS(0) **1**: -8.71, **2**: -10.12
NICS(1) **1**: -7.07, **2**: -11.04

3-21g
NICS(0) **1**: -8.29, **2**: -8.91
NICS(1) **1**: -7.45, **2**: -10.83

6-31g(d)
NICS(0) **1**: -8.11, **2**: -9.81
NICS(1) **1**: -6.79, **2**: -10.87

3-21g
NICS(0) **1**: -6.23, **2**: -8.39
NICS(1) **1**: -5.18, **2**: -10.45

Fig. S9 Calculated NICS (0) and NICS (1) values for BTBT, BSBS, and BTeBTe. Note that the results are almost identical for BTBT and BSBS with different basis sets

10. Ratio of intermolecular contacts in Hirshfeld surfaces analysis

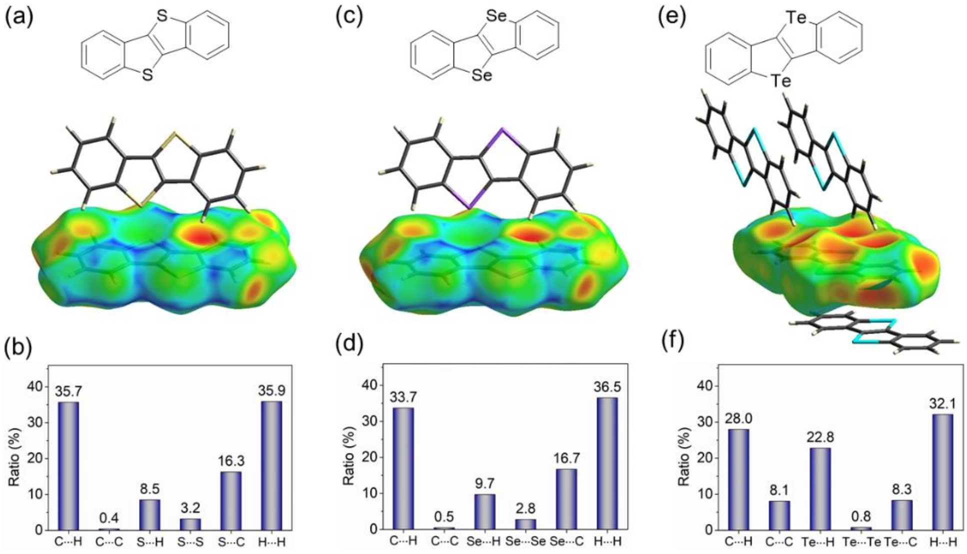

Fig. S10 Ratio of intermolecular contacts in the Hirshfeld surface analysis of BTBT, BSBS, and BTeBTe.

11. Intermolecular interaction energies of various dimers in the packing structures of BTBT and BSBS

Table S1. Intermolecular interaction energies (kcal mol^{-1}) of dimers in the packing structures of BXBXs.$^{a)}$

Compound		E_{es}	E_{ex}	E_{ind}	E_{disp}	E_{total}
BTBT	Edge-to-face	−3.89	8.67	−0.98	−15.03	−11.24
	Edge-to-edge	−4.47	7.86	−0.85	−10.89	−8.35
BSBS	Edge-to-face	−4.95	10.37	−1.08	−15.54	−11.20
	Edge-to-edge	−5.26	8.88	−0.75	−10.85	−7.97

$^{a)}$ Obtained from zeroth-order symmetry-adapted perturbation theory (SAPT0) calculations with aug-cc-pVDZ basis. E_{es}, E_{ex}, E_{ind}, E_{disp}, and E_{total} are electrostatics, exchange, induction, dispersion, and total intermolecular interaction energy, respectively. $E_{\text{total}} = E_{\text{es}} + E_{\text{ex}} + E_{\text{ind}} + E_{\text{disp}}$.

12. Theoretical mobilities

In the conducting layer of BTBT and BSBS, there are three types of hopping dimers, T_p (parallel dimers, edge-to-edge direction), T_1 and T_2 (transverse dimers, edge-to-face direction). The reference axis is along the T_p hopping path, and the angles (θ) between the hopping paths (T_p, T_1 and T_2) to the reference axis are extracted from the crystal structure. To a specific conducting channel, with an angle (φ) to the reference axis, the angle between each hopping path and the conducting channel can be calculated as (ϕ). Thus, the projection of the transfer integrals to the conducting channel from each hopping path can be calculated from ϕ, which gives the combined hopping along the conducting channel, and the anisotropic mobilities referring to the reference axis can be calculated.[S2]

The electronic hopping rate (k_{ET}) is given by the Marcus-Hush equation (1):

$$k_{ET} = \frac{4\pi^2}{h} \frac{1}{\sqrt{4\pi\lambda k_B T}} t^2 \exp\left(-\frac{\lambda}{4k_B T}\right) \qquad (1)$$

where λ is the reorganization energy, t is the transfer integral, and T is the temperature (300 K in this calculation); h and k_B is the Planck and Boltzmann constant, respectively.

The hopping probability regarding to each hopping path can be calculated as by equation (2):

$$13.\ P_i = \frac{k_{ETi}}{\sum_i k_{ETi}} \qquad (2)$$

where i represents a specific hopping pathway.

Considering in this calculation the charge carrier mobility is calculated along a specific direction, thus the charge carrier transport is a one dimentional behavior. The diffusion coefficient D of the charge carriers can be calculated by equation (3):

$$\mathrm{D} = \frac{\sum_i k_{ETi} r_i^2 P_i}{2} \qquad (3)$$

where r_i represents the hopping distance (the distance between the centroids of the dimers).

The drift mobility of charge carriers was derived from the Einstein relation shown in equation (4):

$$\mu = \frac{e}{k_B T} D \qquad (4)$$

where e is the electronic charge.

The projection of all the hopping paths and leads to the charge carrier mobility (μ_φ) along a specific conducting channel as:

$$14.\ \mu_\phi = \frac{e}{2k_B T} \sum_i k_{ETi} r_i^2 P_i \cos^2(\theta_i - \phi) \qquad (5)$$

For BTBT, μ_φ is as:

$$\mu_\phi = 0.008\cos^2(53.97 - \phi) + 0.008\cos^2(53.97 + \phi) + 0.842\cos^2(\phi) \qquad (6)$$

For BSBS, μ_φ is as:

$$\mu_\phi = 0.030\cos^2(54.41 - \phi) + 0.030\cos^2(54.41 + \phi) + 2.451\cos^2(\phi) \qquad (7)$$

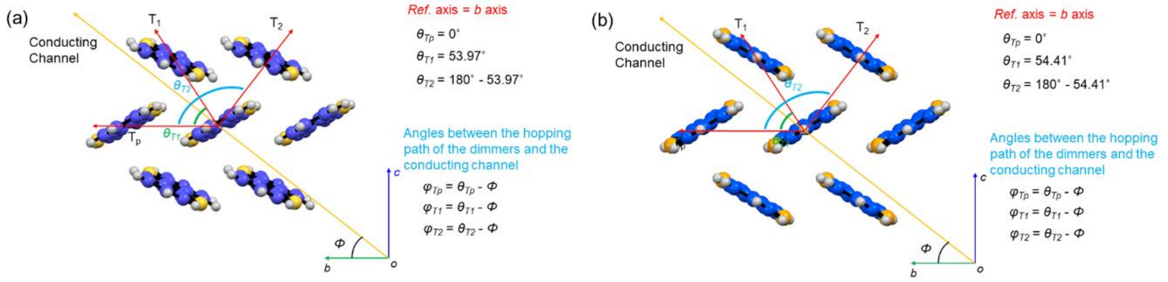

Fig. S11 Illustration of projecting different hopping paths to a specific conducting channel in the molecular layers of (a) BTBT, (b) BSBS.

13. Ionization potentials of BTBT, BSBS, and BTeBTe

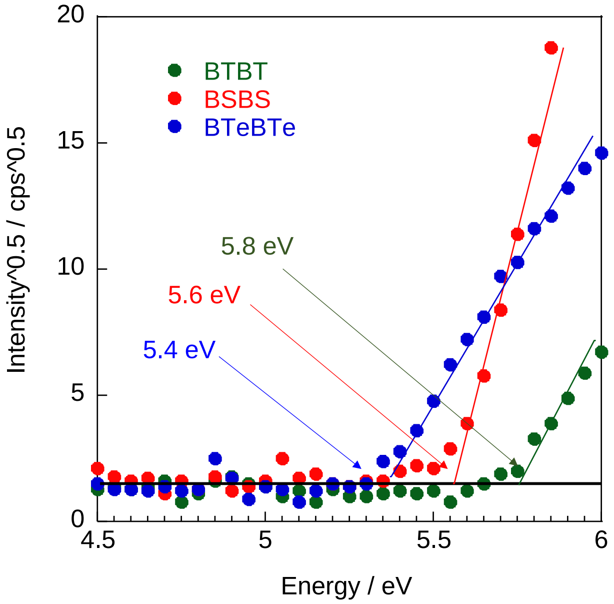

Fig. S12 Photoelectron spectroscopy in air measured for powder samples of BTBT, BSBS, and BTeBTe.

14. Band structures of BTBT, BSBS, and BTeBTe

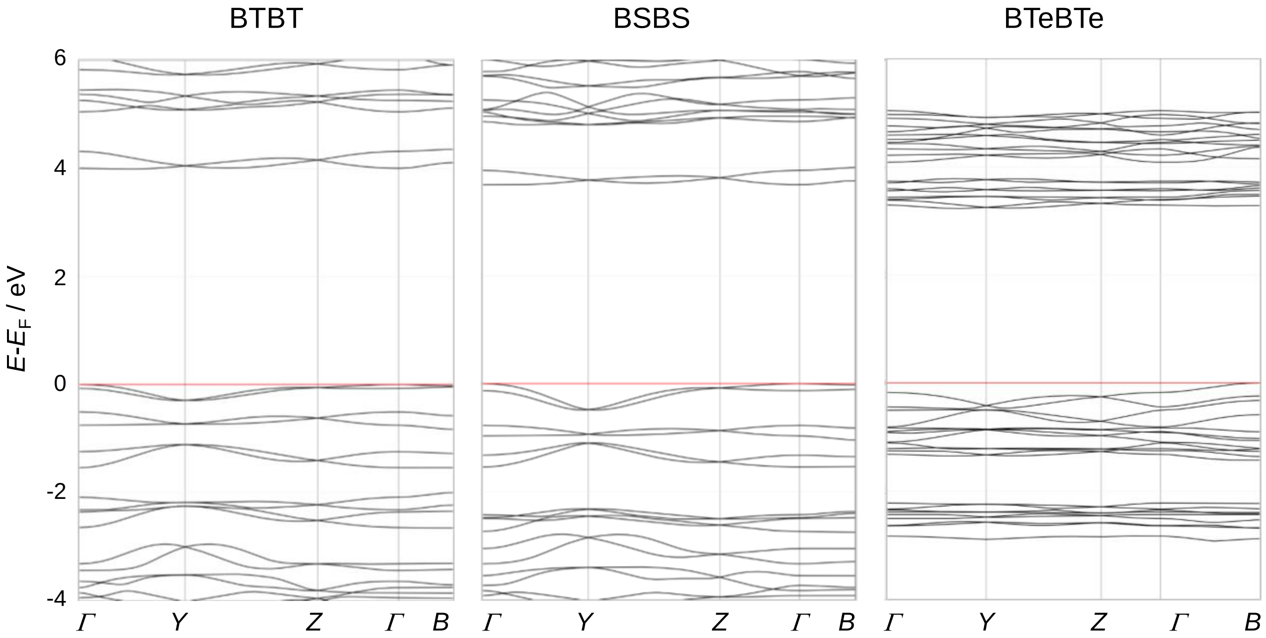

Fig. S13 The DFT-calculated band structures of BTBT, BSBS, and BTeBTe. The reciprocal coordinates of the high-symmetry points are: *Γ* = (0 0 0), Y = (0 1/2 0), Z = (0 0 1/2), *B*= (1/2 0 0).

15. Estimation of carrier effective masses

The effective mass (m^*) at the band extrema in the Γ-Y direction can be expected by using the parabolic fitting combined with the following equation,

$$\frac{1}{m^*} = \frac{1}{\hbar^2}\frac{d^2E(k)}{dk^2}$$

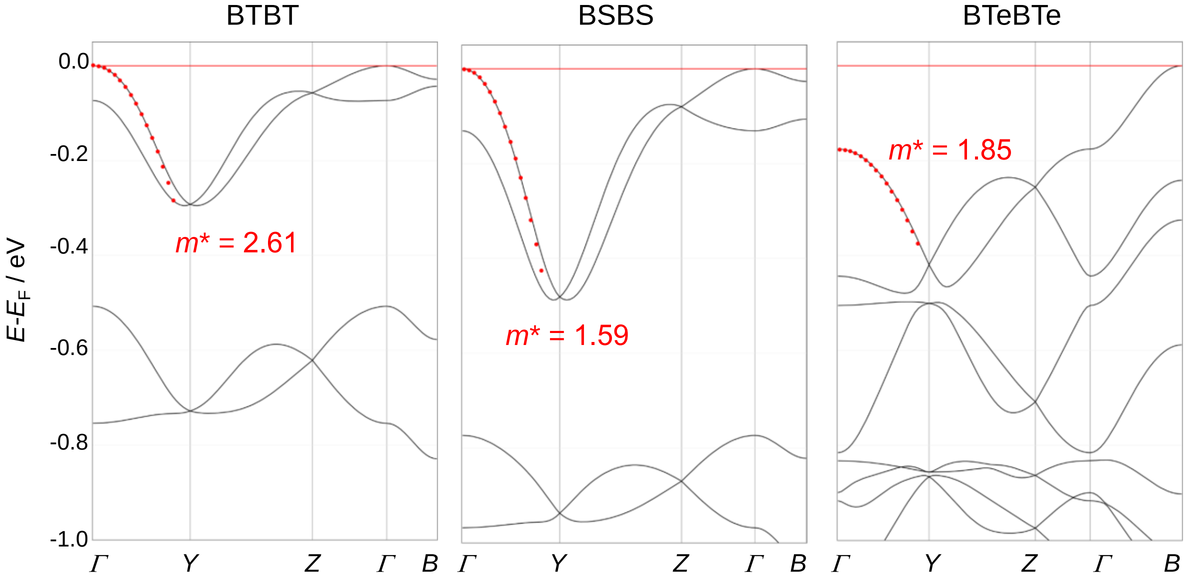

Fig. S14 Parabolic fitting of the band extrema in the Γ-Y direction and estimated m^*. Red dots represent the results of fittings.

16. References

S1 Rigaku Cooperation crystal structure analysis package, https://www.rigaku.com/ja/products/protein/cs.

S2 S.-H. Wen, A. Li, J. Song, W.-Q. Deng, K.-L. Han and W. A. Goddard, *J. Phys. Chem. B*, 2009, **113**, 8813-8819.

S3 M. Z. S. Flores, V. N. Freire, R. P. dos Santos, G. A. Farias, E. W. S. Caetano, M. C. F. de Oliveira, J. R. L. Fernandez, L. M. R. Scolfaro, M. J. B. Bezerra, T. M. Oliveira, G. A. Bezerra, B. S. Cavada and H. W. Leite Alves, *Phys. Rev. B*, 2008, **77**, 115104.